Linear Island Chains in the Pacific: Result of Thermal Plumes or Gravitational Anchors?

HERBERT R. SHAW

U.S. Geological Survey, Washington, D.C. 20244

EVERETT D. JACKSON

U.S. Geological Survey, Menlo Park, California 94025

Recent studies of Hawaiian tholeiitic volcanic suites and of xenoliths of deep-seated material beneath Hawaii lead to the conclusion that the source materials are not pyrolitic. Rather, the source materials have average 100 Mg/Mg + Fe ratios of about 82 and average densities of about 3.30 g cm^{-3}. Residues from melting have average 100 Mg/Mg + Fe ratios of between 84 and 85 and average densities of at least 3.40 g cm^{-3}. The Hawaiian melting anomaly appears to be located in somewhat fractionated asthenospheric source material whose fusion produces material more dense than either its parent or underlying material beneath the asthenosphere. We propose that the volcanic activity at the ends of the Hawaiian, Tuamoto, and Austral chains is not a result of the fortuitous location of thermal plumes but rather is a consequence of shear melting caused by plate motion. Once such melting begins, a dense residuum is formed and sinks. This downwelling ultimately forms gravitational anchors that stabilize the anomalies and cause inflow of fresh partially fractionated parental materials into the source areas for the basalts. These anchors do not drive the plates but rather represent pinning points for melting anomalies at both the top and the bottom of the asthenosphere. Gravitational and bathymetric data, as well as heat flow patterns and anomalous seismic velocities for wave paths through the deep mantle, all appear to support this hypothesis.

The Wilson-Morgan hypothesis that linear volcanic chains and aseismic ridges are formed by thermal plumes under fixed 'hot spots' and that these plumes are associated with the driving mechanism of continental drift has received considerable favorable attention since its development [*Wilson*, 1963; *Morgan*, 1971, 1972*a*, *b*]. It seems apparent that not all of Morgan's originally assumed 20 plumes are of the same kind or quality; indeed, *Kidd et al.* [1973] proposed that there are as many as 150 terrestrial plumes, and *Wilson and Burke* [1973] classified plumes into several categories. We wish to take a conservative stance regarding the plume hypothesis, and we introduce the term 'melting anomaly' in its place to emphasize that unusual volcanic activity may ensue from a variety of processes. We also wish to encourage the idea that individual melting anomalies may arise from different dynamic situations. Indeed, considerable attention has been given to other ideas of melting anomaly origin—propagating fractures [*Betz and Hess*, 1942; *Jackson and Wright*, 1970; *McDougall*, 1971], rheological intrusion [*Green*, 1971], shear melting [*Shaw*, 1973], bumps on the asthenosphere [*Menard*, 1973], and so on. In this paper we propose the idea that the melting anomalies in the Pacific at the ends of linear island chains are relatively fixed, not by thermal plumes that rise from the mantle-core boundary, but rather by gravitational anchors of residual material that, in the case of at least the Hawaiian-Emperor, Line-Tuamoto, and Marshall-Austral chains, have flowed down through the mantle to the core boundary.

We plan to extend the mechanism proposed by *Shaw* [1973] for the origin of the Hawaiian melting anomaly. Shaw proposed that the zone in which plate motion is decoupled from the deeper mantle contains variable gradients of horizontal flow velocities that depend intrinsically on the distribution of a variable melt fraction. The existence of episodic variations in volcanic propagation speeds and volume rates are taken as prima facie evidence of variations in horizontal flow velocities beneath the lithosphere, dependent only on the one assumption that magma production is at least partly controlled by the mechanics of mantle flow. *Shaw* [1973] showed that systematic functional relationships exist between distance of volcanic propagation, volumes of lava extruded, and time and that these relationships are interrelated by feedback processes, applying the phrase conceptually in a manner analogous to the ideas of 'systems analysis' [*Forrester*, 1968]. The principal feedback loop discussed relative to magma production was the relationship between horizontal shear stresses, shear rates, and apparent viscosity as a function of melt fraction, as was proposed by *Shaw* [1969] following the analytic results of *Gruntfest* [1963]. However, other types of feedback were pointed out in *Shaw* [1973], and we add yet another in the present paper. Some general consequences of the thermal feedback model are: (1) melting anomalies of the Hawaiian type are interpreted as mechanical anomalies rather than anomalies of terrestrial heat flow; (2) the asthenosphere is defined kinematically and dynamically by the three-dimensional distribution of flow trajectories influenced by the rates of production and withdrawal of a melt fraction; (3) the thickness of the dynamic asthenosphere varies episodically with rates of melting; (4) horizontal flow velocities in the vicinities of asthenosphere melting anomalies accelerate and decelerate relative to more or less steady velocities of plate motion and mantle counterflow; and (5) the direction of propagation of the geometric center of a melting anomaly relative to the deep mantle tends to be governed by the sign of the vector sum of lithosphere translation and asthenosphere flow, so that a fixed melting spot could in principle be produced by locally symmetrical counterflow.

Data given by *Jackson and Wright* [1970] suggested that the lithosphere beneath Hawaii behaves elastically to depths of about 60 km and that the source region for tholeiitic basalt probably extends to depths of about 100 km. *Shaw* [1973] viewed the region between 60 and 100 km as the zone in which maximum gradients of flow velocities occurred and as the general site of decoupling of lithospheric plate motion from that of the deep mantle. This paper discusses some consequences of this dynamic model viewed according to additional petrologic constraints on compositions and densities of rocks in the asthenospheric source regions. *Jackson and Wright* [1970], *Jackson et al.* [1972], and Jackson and Shaw (unpublished data, 1973) discussed the physical properties and dynamic relations within the rigid lithospheric plate.

Shaw's [1973] model of plate-mantle interaction did not attempt to deal with components of vertical flow implied by density models of the asthenosphere and deeper mantle. Reevaluation of the petrologic data of *Jackson and Wright* [1970] in terms of the dynamic model suggests that the Hawaiian melting anomaly and other melting anomalies at the southeastern ends of the Austral and Tuamoto linear island chains are not maintained by hot spots or thermal plumes but rather are stabilized by gravitational anchors. We propose to examine the effect of 'downwelling' below these melting anomalies and its relationship to global kinematics. We propose the following sequence of events during a melting episode: (1) a melt fraction in the asthenosphere builds up sufficiently to satisfy criteria of extensional failure of the lithosphere; (2) the magma is injected into the lithosphere; intrusion and, commonly, extrusion proceed as a consequence of the uncompensated hydraulic head produced by density contrasts between rock and magma columns; (3) depletion of the melt fraction in the asthenosphere increases the degree of shear coupling between the lithosphere and deeper mantle; (4) shear stresses build up to higher values than the average for steady plate motion because of a tendency to lock the lithosphere-asthenosphere flow boundary at points of melt depletion; (5) the dense residuum formed in this depleted zone during melting begins to sink through underlying source materials; (6) new, partially fractionated, material adjacent to the depleted zone flows in to compensate the volume deficiency produced by the sinking material; (7) shear melting begins to increase in the new material because of anomalous stresses produced by tendencies to retard motions of both lithosphere and asthenosphere near the site of previous melting, relative to the general motions of the entire Pacific plate and underlying mantle; (8) melting rates accelerate in the upper part of the asthenosphere; (9) the new asthenosphere partially melts to tholeiitic liquids and produces refractory residua with relatively high Fe/Mg ratios; (10) shear coupling of lithosphere and mantle rapidly fails, accompanied by a stress drop that occurs just before repetition of step 1, in which (11) the liquid fraction has again built up sufficient pressure to satisfy criteria of extensional failure of the lithosphere. Tests of this model are found in chemical and seismic data on density distributions in the mantle and in data on regional topographic, gravitational, and heat flow distributions, as well as recent discoveries of anomalous seismic wave paths near the core-mantle boundary below Hawaii.

Some Dynamic Implications of Asthenospheric Transport

Asthenospheric flow below the front of the melting anomaly implied by the model of *Shaw* [1973] proceeds, on the average, at about the same rates as plate motion; it was proposed that at times horizontal flow rates in the asthenosphere advance beyond, and at other times lag behind, a fixed position relative to the deep mantle. Shaw described this process as analogous to a throttling point in the mean flow of sublithospheric mantle toward a spreading ridge. This concept does not necessarily conflict with the results of *Schubert and Turcotte* [1972], who argued that a model of one-dimensional counterflow does not predict the observed topography of the ocean floor near trenches (but see section 3 of the appendix). However, in order to maintain continuity of flow across the position of a throttling point, there must be an upward component of flow behind the position of the anomaly (relative to the volcanic propagation direction, northwest in the case of Hawaii and similar chains) and a downward component ahead of the volcanic wave front.

Although the kinematic necessity of vertical transfers in the asthenosphere was evident from accelerations of flow velocities discussed by *Shaw* [1973], the physical basis for two-dimensional flow was not explicitly included in his thermal feedback model. One important implication of the vertical components of flow vectors is that the local rate of viscous dissipation is smaller and extends over a greater depth range at positions ahead of and behind the throttling point (again we emphasize that directions are defined according to asthenospheric flow and volcanic propagation; that is, 'ahead' refers to positions southeast of the Hawaiian and other ridge fronts that are kinematically similar). Therefore incipient stages of partial melting extend to greater depths behind the front of maximum tholeiitic melting, which is approximately below the front of volcanic propagation, and these materials are carried up as the flow instability approaches the culminating stages of a melting episode [*Shaw*, 1973]. This effect augments whatever initial gradients of temperature and melting points that were responsible for the development of melting instabilities at various locations below the Pacific lithosphere.

The vertical component of asthenospheric flow ahead of the melting front carries some of the residual materials that are left after the extraction of the tholeiitic fractions downward and again reduces the heating rates per unit volume because of the reduced shear rates. We note, however, that the total heating rate below a given point at the surface is given by the integral of local volumetric rates [*Shaw*, 1973, p. 1518] and that these total rates remain, on the average, roughly constant over the Pacific mantle, as in models discussed by *Schubert and Turcotte* [1972]. That is, the wave front of tholeiitic melting is not a hot spot insofar as lateral gradients of surface heat flow are concerned.

The upward transport behind the melting front and downward transport ahead of this front are also augmented by buoyancy effects. Incipient melting generally tends to decrease the density, and the eventual removal of tholeiitic fractions by volcanism tends to increase the density of the refractory residuum.

The remainder of this paper considers the question of density changes in the asthenosphere source region and their implications on downwelling ahead of the melting front.

Density Models in the Tholeiitic Source Region

The presence of seismic tremor at depths of 40–60 km directly beneath the summit area of Kilauea volcano [*Eaton*, 1962, 1967; *Koyanagi and Endo*, 1971] is generally accepted as direct

TABLE 1*a*. Bulk Chemical Composition of Mantle Materials beneath Hawaii

	Dunite* D102224 66ULUP-25	Dunite† D102103 66KAP-1	Garnet Lherzolite§ D102100 66SAL-1	Calculated Mantle‖
SiO_2	38.78	39.33	44.82	43.03
Al_2O_3	0.91	0.85	8.21	4.34
Fe_2O_3	3.00	1.05	2.07	...
FeO	11.48	12.96	7.91	12.67
MgO	43.46	44.90	26.53	35.00
CaO	0.05	0.18	8.12	3.06
Na_2O	0.10	0.04	0.89	0.65
K_2O	0.00	0.01	0.03	0.10
H_2O^+	n.d.	0.00	0.11	...
H_2O^-	0.13	0.00	0.15	...
TiO_2	0.08	0.05	0.52	0.60
P_2O_5	0.01	0.01	0.04	0.06
MnO	0.19	0.19	0.19	0.18
CO_2	n.d.	0.01	0.01	...
Cl	n.d.	0.00	0.00	...
F	n.d.	0.00	0.01	...
S	n.d.	0.01	0.04	...
Cr_2O_3	1.00	0.38	0.20	0.31
NiO	n.d.	0.29	0.20	...
Subtotal	99.19	100.26	100.05	100.00
Less O	0.00	0.01	0.02	...
Total	99.19¶	100.25	100.03	100.00
100 Mg/Mg + Fe	84.5	85.2	82.9	83.1

*Dunite xenolith, Ulupau Head, Oahu [*Jackson and Wright*, 1970].
†Dunite xenolith, Hualalai volcano, Hawaii [*Jackson and Wright*, 1970].
§Garnet lherzolite xenolith, Salt Lake crater, Oahu [*Jackson and Wright*, 1970].
‖Calculated composition and mode of Mauna Loa mantle [*Wright*, 1971].
¶Only a small sample was available for analysis.

evidence of movement of magma from an upper mantle source into the volcanic edifice manifest at the surface. The product of this melting, currently being erupted at Kilauea and Mauna Loa volcanoes, and observed in the cores of older eroded volcanoes, is tholeiitic basalt. *Jackson and Wright* [1970] argued that the residuum from tholeiitic melting was dunite with an average 100 Mg/Mg + Fe ratio of about 86.0. They based this contention on the prevalence of deformed, partially syntectonically recrystallized dunite tectonite xenoliths in lavas younger than tholeiites, which appear to have incorporated these xenoliths in their passage through former tholeiitic source regions. In the case of the Koolau shield, they showed an areal distribution of these dunite xenoliths in younger lavas that is spatially related to the old Koolau tholeiitic eruption center. Chemical and modal analyses of two of these xenoliths

TABLE 1*b*. Modes and Densities of Mantle Materials beneath Hawaii

Minerals	66ULUP-25	66KAP-1	66SAL-1	Calculated Mantle
Olivine	95.6	97.7	28.7	60.12
Orthopyroxene	...	0.1	12.1	17.72
Clinopyroxene	1.3	0.8	33.5	15.79
Phlogopite	...	...	...	...
Amphibole	...	...	...	4.85
Oxide minerals	3.1	1.4	3.6	1.02
Sulfide minerals	...	...	tr	...
Garnet	...	...	22.1	...
Apatite	...	...	tr	0.14
Rutile	...	...	...	0.37
Total	100.0	100.0	100.0	100.01
opx/opx + cpx	...	0.11	0.27	0.53
Density, g cm^{-3}	3.36	3.39	3.22*	...
100 Mg/Mg + Fe of olivine	85.4†	87.7†	83.8†	83.8

*The published value of density of this rock was 3.33 g cm^{-3}, a typographical error not previously noted. The original value of 3.22 g cm^{-3} has been redetermined.
†Determined by microprobe analysis by M. H. Beeson.

TABLE 2. Densities and Magnesium-Iron Ratios of Potential Mantle Residua from the Melting of Hawaiian Tholeiites

Sample Number	Density, g cm^{-3}	Rock Type	Location	100 Mg/Mg + Fe* of olivine
65 KAP-16	3.31	Dunite	Hualalai	85.5
68 KEA2-1	3.29	Dunite	Mauna Kea	86.5
67 KEA2-30	3.27	Dunite	Mauna Kea	85.5
63 KAP-10	3.35	Dunite	Hualalai	85.5
63 MK-10	3.32	Dunite	Mauna Kea	84.5
67 KEMO-3	3.30	Dunite	Mauna Kea	84.5
70 KAP-1	3.36	Dunite	Hualalai	85.5
70 KAP-2	3.35	Dunite	Hualalai	81.5
66 KAP-11	3.42	Dunite	Hualalai	81.5

*Determined by Keith Bargar by X ray procedures [*Hotz and Jackson*, 1963].

are given in Tables 1*a* and 1*b*. Density measurements on eleven dunite xenoliths of this type range from 3.27–3.42 g cm^{-3}, and the average is 3.34 g cm^{-3} (Tables 1 and 2). The 100 Mg/Mg + Fe ratios of the olivine in these dunites, which are essentially equivalent to whole rock values, range from 81.5 to 86.5 and average 84.6. (Densities were determined on rock chips weighing between 20 and 500 grams on a Dec-O-Gram density balance. The dunites are somewhat friable rocks, and measured densities fall 0.01–0.10 g cm^{-3} below the olivine density curves of either *Deer et al.* [1962] or *Robie et al.* [1967], in spite of the fact that the dunites contain several percent spinel. Calculated zero-pressure density ρ_0 for olivine of 100 Mg/Mg + Fe = 84.6 would be between 3.40 and 3.43 g cm^{-3}, depending on the data used.)

Wright [1971] independently calculated the olivine phenocryst compositions of Kilauean and Mauna Loan undifferentiated lavas as 86.2 and 87.5 100 Mg/Mg + Fe, respectively. These values are in fair agreement with those of the dunite xenoliths, and whether the xenoliths are residua of partial melting, as *Jackson and Wright* [1970] contended, or deformed cumulates, as *O'Hara* [1968*a, b*] believed, is unimportant to the fact that the early phenocrysts of the tholeiites are compositionally as well as spatially linked to the dunite xenoliths. Given the composition of the tholeiitic lavas and of their deep-seated olivine-rich residua (or olivine-rich fractionation products), *Jackson and Wright* [1970] and *Wright* [1971] contended that parental material must lie on control lines connecting the chemical compositions of these two rock types.

Jackson and Wright [1970] found the most suitable parental material among certain garnet lherzolite xenoliths (the chemical analysis and mode of their 'parent' are given in Tables 1*a*, *b*). Measured densities of six Hawaiian garnet lherzolites (Tables 1 and 3) range from 3.14–3.34 g cm^{-3}, and average 3.27 g cm^{-3}. (Again, calculated zero pressure densities for these rocks would probably be higher than those measured, although we cannot at this time say how much. In general, however, these samples are considerably more coherent than the dunites, and measured densities are probably nearer true values.) The 100 Mg/Mg + Fe ratios of these rocks range from 76.9 to 84.6 and average 82.0. The 100 Mg/Mg + Fe values of the olivines in these rocks (Table 3) are practically identical with those of the whole rocks.

Both the whole rock and olivine magnesium-iron ratios are consistent with the idea that these rocks form a range of source materials for the range of more magnesian dunite residua and the range of more ferroan tholeiitic melt products. In spite of the fact that all these garnet lherzolites contain 5–20% rather pyrope-rich garnet and that they contain more iron-rich olivine than the dunites, the abundance of aluminous pyroxenes causes bulk density of the rocks to average 0.07 g cm^{-3} less than that of the dunites.

The garnet lherzolite xenoliths, although suitable parental material for many major ele-

TABLE 3. Densities and Magnesium-Iron Ratios of Potential Mantle Source Rocks for Hawaiian Tholeiites

Sample Number	Density, g cm^{-3}	Rock Type	Location	100 Mg/Mg + Fe* (Rock)	100 Mg/Mg + Fe† (Olivine)
69 SAL-97	3.33	Garnet lherzolite	Salt Lake Crater, Oahu	84.6	86
69 SAL-121	3.14	Garnet lherzolite	Salt Lake Crater, Oahu	84.2	83.5
69 SAL-96	3.30	Garnet lherzolite	Salt Lake Crater, Oahu	81.3	81.5
69 SAL-106	3.34	Garnet clinopyroxenite	Salt Lake Crater, Oahu	76.9	76
69 SAL-89	3.28	Garnet lherzolite	Salt Lake Crater, Oahu	82.3	81.5

*From unpublished chemical analyses, Elaine L. Brandt, U.S. Geological Survey analyst.
†Determined by Keith Bargar by X ray procedures [*Hotz and Jackson*, 1963].

ments, are obviously depleted in potassium, phosphorus, water, and the large rare earths. *Wright* [1971] therefore took a different approach and calculated the chemical composition and mode of Mauna Loan parental material at a given MgO content (Tables 1*a* and 1*b*). The olivine of Wright's calculated parental material has a 100 Mg/Mg + Fe ratio of 83.8, and the whole rock value is 83.1. The range of 100 Mg/Mg + Fe of 100 Kilauean and Mauna Loan olivine controlled tholeiites, calculated from *Wright* [1971], is 49.0–79.0, but the average is 57.2, considerably lower than *Green's* [1971, p. 723] ranges of 63–73 for 'basalts of world-wide occurrence.' Although it is not feasible to calculate the density of Wright's parental assemblage, it is apparent that the presence of such large quantities of aluminous pyroxenes and amphibole (Table 1*b*) would result in an assemblage density less than that of dunite with a 100 Mg/Mg + Fe ratio of 84.6.

It seems clear from two different sets of data and two approaches to the analysis of those data that the Hawaiian tholeiitic parental material cannot be pyrolite [*Ringwood*, 1966; *Green and Ringwood*, 1967]. Pyrolite has a 100 Mg/Mg + Fe ratio of 89.0 [*Green*, 1971] and would yield residua (or early phenocrysts) with even higher Mg/Mg + Fe ratios; it also would yield lavas with higher ratios than those observed at Kilauea and Mauna Loa. It may well be that the average composition of the oceanic mantle is pyrolitic; it may even be that the source materials for mid-oceanic ridge basalts away from melting anomalies such as Iceland are pyrolitic. The source material for Hawaiian tholeiites, however, appears to be too overly enriched in iron and in large ion constituents such as potassium, water, phosphorus, and the larger rare earths for it to be a result of the static melting of material of pyrolitic composition.

Seismic evidence places the origin of Hawaiian tholeiitic magmas at depths at least as great as 60 km. Their source is therefore near the base of the oceanic lithosphere and in the asthenosphere, whether directly by shear melting, as we believe, or as a result of the intrusion of asthenospheric materials into the lithosphere as *Green* [1971] and *McDougall* [1971] believe. *Spetzler and Anderson* [1968] and *Anderson et al.* [1972] considered the relation of the asthenosphere to the seismic low-velocity zone and gave evidence that a two-phase mixture of crystalline material and liquid may exist in the region we consider to be the source of melting. We see no reason to suppose that the upper mantle, which is so seismically heterogeneous, is compositionally homogeneous. Instead, the dynamic processes of plate motion that created the asthenosphere may well have fractionated it, and, in the Hawaiian region and perhaps generally across the Pacific, it may be enriched in iron, potassium, water, phosphorus, and the large rare earths with respect to both the base of the lithosphere and the mantle below the asthenosphere. Whether or not the entire low-velocity zone is enriched in these constituents, we propose that the shear melting process itself enriches source material flowing into the site of a melting anomaly by enhancing lateral migration of low melting point constituents. The difference between this type of material and that below spreading ridges may be largely a consequence of dynamic effects, although lateral heterogeneities in mantle composition may also be a factor.

Our best estimate of the nature of the source material for Hawaiian tholeiitic basalt is that it consists basically of garnet lherzolite, quite probably containing a small liquid fraction enriched in large ions, that it has a bulk 100 Mg/Mg + Fe ratio of about 82, and, if a fluid phase is present, that it has an average zero pressure density ρ_0 of no more than 3.30 g cm^{-3}. The residuum of the melting process is dunite with an average 100 Mg/Mg + Fe ratio of about 84.6 and an average zero pressure density ρ_0 of at least 3.40 g cm^{-3}.

DYNAMIC ANALYSIS OF GRAVITATIONAL ANCHORS

Sinking rates of dense bodies. Given that the density of residual materials in the source region is greater than that of the parental material, sinking of this residuum is inevitable unless the underlying mantle has a high enough yield strength to prevent downwelling. *Morgan* [1965] showed that the stresses at the boundaries of a spherical or cylindrical 'sinker' with a diameter of the order of 100 km easily exceed any likely values of a yield strength for mantle materials [cf. *Shaw et al.*, 1968, p. 259]. Flow laws for dunitic materials and estimates of effective viscosities for solid state creep in the mantle substantiate this conclusion [*Weertman,* 1970; *Goldreich and Toomre,* 1969; *Dicke,* 1969]. The above studies suggest an effective viscosity of the order of 10^{23} poises for the deep mantle.

(In this simplified discussion we simply assume that the viscosity is constant. However, if a power law model such as that described by *Weertman* [1970] is applied for boundary stresses given by the density contrast and dimensions of sinkers discussed by *Morgan* [1965], the effective viscosity could be even smaller. For example, if the radius of the sinker is 100 km and $\Delta\rho \simeq 0.05$, the average boundary stresses are of the order of 100 bars. From *Weertman* [1970, Figure 5] the effective viscosity would be 10^{23} poises for $T = T_m/2$, where T_m is the melting temperature, and 10^{14} poises for $T = T_m$. *Weertman* [1970, Figure 7] suggests that T ranges from T_m to $T_m/2$ between the asthenosphere and core-mantle boundary. If so, the effective viscosities for the sinker would never exceed 10^{22} poises.)

The sinking rate of a spherical body, as given by *Morgan* [1965], is found from the equation

$$U = \frac{2ga^2\,\Delta\rho}{9\eta}\,\frac{1}{1 + (3/4)e + (9/16)e^2 + \cdots} \tag{1}$$

where a is the radius of the sphere, $\Delta\rho$ is the density contrast, η is the effective viscosity of the mantle, and e is the ratio a/D for D, the depth of the center of the sphere below the earth's surface. The first term on the right side corresponds to Stokes's law, and the second term is a correction for the effect of proximity to the surface. Equivalent corrections for boundary effects are given in many other studies [e.g., *Happel and Brenner,* 1965, pp. 329–331]. For a radius of the order of 100 km, a density contrast $\Delta\rho \simeq 0.05$ g cm^{-3}, and a viscosity of 10^{22} poises, the sinking velocity is of the order of 1–3 cm/year, depending on depth below the surface. These rates are of the same order of magnitude as the average propagation rates of the Hawaiian ridge during its earlier stages of growth [*Shaw,* 1973, Table 2].

Vertical density currents. The growth of vertical density currents in a fluid was documented in a remarkable series of experiments and observations by *Bradley* [1965, 1969]. He showed that when an aggregate of particles was deposited at the interface between two fluids (aqueous solutions), of which the lower fluid was the more dense, the resulting slurry (denser than either of the homogeneous fluids) first tended to spread out, but then very rapidly formed unstable lobes that coalesced into a stream tube that descended to the bottom of the container. Figures 1*a* and 1*b* are reproductions of his sketches of this process. Bradley found that after the initial stages of development the rate of descent of the leading end of of the suspension cloud was remarkably constant. Unfortunately, he gave no estimates of the bulk density of the suspension. If it is assumed that the velocity is mainly governed by the diameter of the stream tube and the density contrast, the density contrast between solution and suspension for the case of Figure 1 (the reported velocity was about 1 cm sec^{-1}) would have been about 10^{-4} g cm^{-3}, under the assumption of laminar flow. This contrast seems rather small, judging from the description of the manner in which the suspension was formed, and it seems likely that the velocity was partly influenced by tendencies for turbulent instability, as is shown in other examples illustrated by Bradley.

In an independent experiment, one of us (Shaw, unpublished data, 1966) observed the growth of a vertical density current of small glass beads (diameters 5–60 μm) in a viscous silicone fluid (viscosity 10^3 poises). In this case the flow was demonstrably laminar (the diameter of the stream tube was about 0.2 cm). Measured velocities over a distance of 13 cm (length/diameter ratio > 50) were between 2×10^{-4} and 2×10^{-5} cm sec^{-1}, decreasing with time because the rate of supply of suspension diminished and the tube diameter became visibly attenuated (roughly by a factor of 3). The average density of the suspension was estimated to be about 1.1 g cm^{-3} (on the basis of the initial concentration of particles), giving a density contrast of about 0.1 g cm^{-3}. The Stokes velocity for a sphere of the above diameter and density in the same fluid would be about 2×10^{-4} cm sec^{-1}.

The approximate agreement with Stokes's law is substantiated by the results of *Happel and Brenner* [1965, p. 156] for the resistance forces on cylinders and prolate spheroids translated parallel to the axis of revolution. Generally speaking, the resistance force increases with the length, compared with that for a sphere of the same diameter, but the buoyancy force also increases and the sinking velocity of a rigid vertical cylinder would be greater than that of a sphere of the same diameter. In the case of a cylindrical density current, however, the velocity is mainly governed by the rate of supply of the suspension. If the radius and density contrast were constant, the velocity would increase as the length became greater, but this would require an increasing rate of supply to maintain constancy of density contrast and radius. Therefore, with a constant

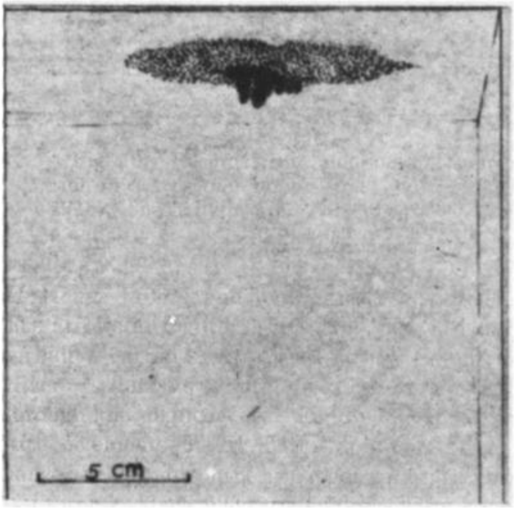

Fig. 1*a*.

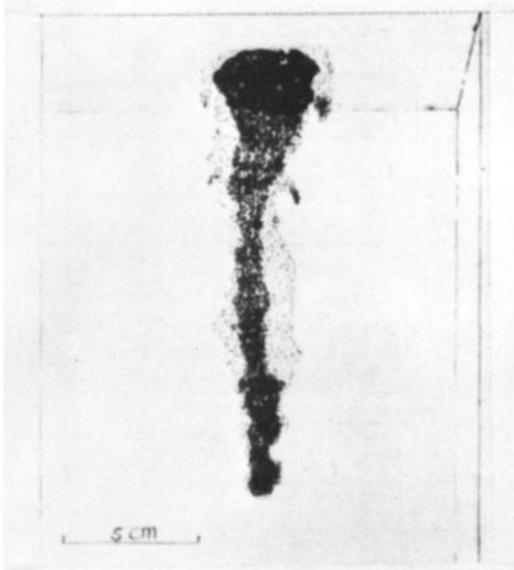

Fig. 1*b*.

Fig. 1. Growth of a vertical density current in experiments by *Bradley* [1965]. (*a*) 'Several small vertical density currents forming on the underside of a disk of particles suspended for an instant at the interface between dilute saline solution and an overlying layer of distilled water. A moment later these tiny density currents merged into one current, which entrained the remainder of the particles above the chemocline' [*Bradley*, 1965, Figure 2, p. 1424]. (*b*) 'A later stage of the currents . . . , showing the small vertical density currents merged into a single current, in which some of the original filaments may be seen. The diffused margin of this density current contrasts sharply with the smooth walls of faster-flowing vertical density currents' [*Bradley*, 1965, Figure 3, p. 1424]. (Figures and legends copyright 1965 by the American Association for the Advancement of Science. Reproduced with permission.)

supply rate, the radius (or, in liquid suspensions, perhaps the concentration of particles) will decrease, and this will tend to maintain a more or less steady rate of descent, in agreement with the observations of *Bradley* [1965] and of Shaw (unpublished data, 1966).

THREE-DIMENSIONAL FLOW MODEL FOR HAWAII

In order to focus on the interactions of various dynamic mechanisms that operate in the vicinity of a melting anomaly, we have drawn a highly schematic picture of the mantle in Figure 2, showing streamlines of asthenospheric flow near the top of a vertical stream tube. We emphasize that the position of the anchor relative to surface topography depends on evaluation of several factors that influence the pressure distribution in the mantle (some of the factors are discussed separately in the appendix). Numerical modeling in three dimensions will be required to test the implications of the model as it is conceived in the qualitative sketch. The three-dimensional trajectories of flow between the site of the melting anomaly and the top of the density current locked in the deep mantle are undoubtedly very complex. A general mental picture of the flow can be obtained, however, by imagining a layer of viscous liquid flowing over a plane surface that contains an aperture permitting some of the

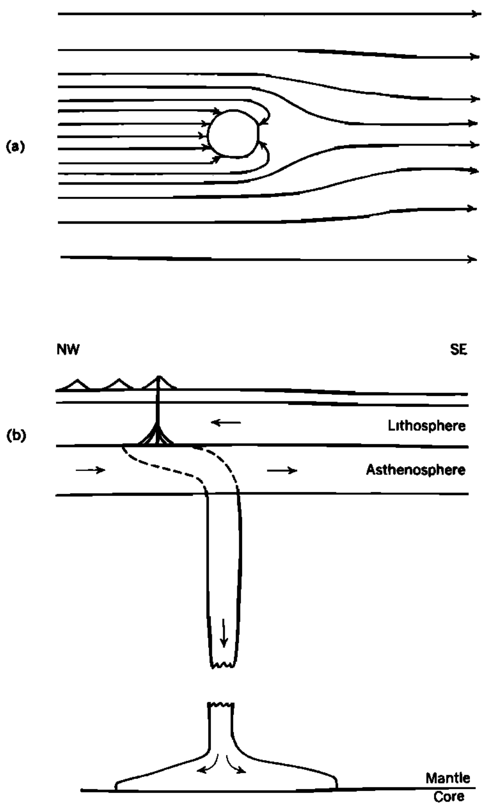

Fig. 2. Schematic views of downwelling of dense residua from tholeiite melting. (*a*) Plan view showing hypothetical flow lines in the asthenosphere along a horizontal plane taken at a time near the culmination of a melting episode. (*b*) Vertical section showing offset between position of melting anomaly feeding surface volcanism and pinning point where dense residua penetrate and become fixed relative to the deep mantle. The distance of offset is uncertain and is expected to vary during a volcanic episode. Penetration of the density current into the mantle below the asthenosphere acts to position the melting anomaly by influencing flow rates of undepleted asthenosphere that melts according to the shear mechanism of *Shaw* [1973]. The diameter of the density current varies with depth depending on melting rates and rate of production of residual fractions.

liquid to leak out the bottom. In slow viscous flow, the velocities directly upstream from the aperture are increased, whereas downstream there is a local region of backflow, a stagnation point, and gradually increasing velocities. At some distance from the aperture in both the flow direction and directions perpendicular to it the flow field is only slightly disturbed if the aperture is small relative to the horizontal dimensions of the stream. If there is no translation of the viscous layer, of course, the flow pattern is simply that of a simple orifice [*Happel and Brenner*, 1965, p. 153].

The model in Figure 2 represents a snapshot at a time long after the density current became locked to the deep mantle. Early in the development of such a system, before the sinking residuum has penetrated below the asthenosphere, the density current is not pinned to the mantle. At this stage the melting anomaly can be expected to migrate relative to the deep mantle, and the propagation direction of related volcanism could be either forward or backward relative to the sign conventions for the Hawaiian ridge, depending on relative velocities of the lithosphere and asthenosphere. The same situation could arise if an anchor, having reached the deep mantle, became decoupled from its source.

The variation in diameter of the stream tube shown in Figure 2 corresponds to variations in the melting rate, because times of high volcanic production rate increase the supply rate of the dunitic density current and consequently its local sinking velocity. Since this velocity also influences local horizontal velocities in the asthenosphere, these variations represent an additional feedback loop that governs the volcanic episodes. If the supply rate subsequently diminishes or if the sinking rate becomes too great, the upper part of the stream tube becomes attenuated and the velocities and melting rates in the asthenosphere are diminished. Thus thermal feedback in the asthenosphere is expected to interact with pulsations of flow or with kinematic waves moving down along the density current to the depth of stable stratification. This depth will be the core-mantle boundary if phase transitions do not change the sign of buoyancy forces.

GEOPHYSICAL TESTS

Gravity. We wish to consider the influence of the density current on gravity from the viewpoints of (1) free-air anomalies and (2) the gravity field determined from satellite orbits. The free-air anomalies will be more strongly influenced by density distributions and dynamics near the earth's surface, whereas the geoidal

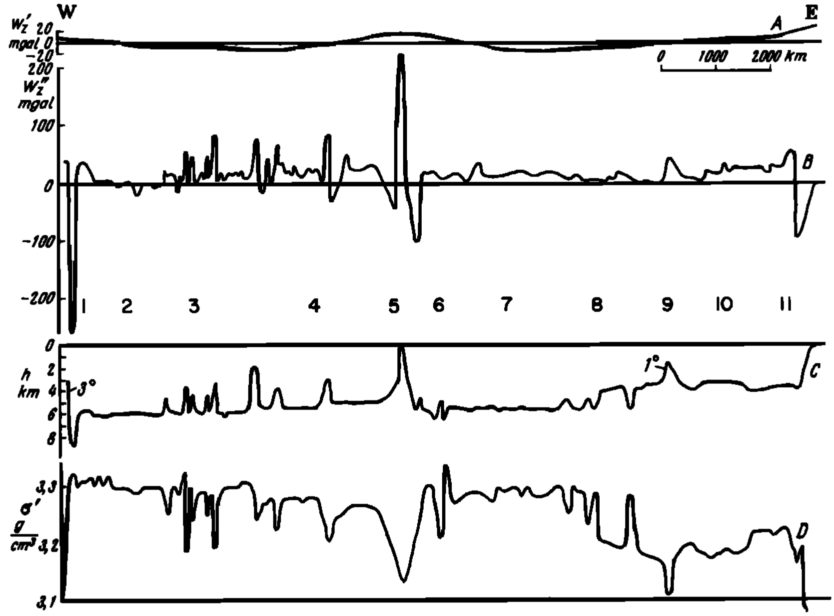

Fig. 3. Interpretation of gravity data along a profile across the Pacific [*Uspensky*, 1972, Figure 3]. 'Gravity profile across the Pacific Ocean. Curve A shows regional gravity anomalies of the first order from satellite observations; curve B, residual gravity free-air anomalies; curve C, ocean-floor topography; curve D, variation of apparent density of the combined layer of the crust and mantle to a depth of 50 km below sea level. Numbers refer to regions studied. 1, Japan trench; 2, northwest Pacific Ocean basin; 3, mid-Pacific mountains; 4, Necker ridge; 5, Hawaiian ridge; 6, fracture zone; 7, east Pacific Ocean basin; 8, Clarion fracture zone; 9, Shimada bank; 10, east Pacific ridge; 11, Middle America trench' [*Uspensky*, 1972, p. 6320].

contours reflect more general balances deeper in the mantle [*Stacey*, 1969, p. 51].

As mentioned in the appendix, section 2, the analyses by *Morgan* [1965] suggest that regions of horizontal convergence should be associated with negative free-air anomalies, other things being equal. Figure 3 shows gravity profiles across the Pacific, reproduced from *Uspensky* [1972, Figure 3]. Strong negative free-air anomalies are found at the trenches. The Hawaiian ridge is associated with a very sharp positive anomaly but is flanked on both sides by negative anomalies nearly as large as those found at trenches. If the positive anomaly is associated with mass distributions in the lithosphere, subtraction of that anomaly would leave a very large negative anomaly centered slightly east of the topographic maximum. However, it is well known in gravity studies, and it was emphasized by *Morgan* [1965] that free-air anomalies are produced by many complex factors that obscure their dynamic interpretation.

Figure 3 also gives the regional anomalies from satellite observations showing a broad positive anomaly nearly centered over Hawaii; this anomaly is shown in more detail on the contour maps of *Kaula* [1972]. *Morgan* [1972*a*, p. 206] stated that the anomaly substantiates the existence of a thermal plume under Hawaii, giving the explanation, 'Such gravity highs are symptomatic of rising currents in the mantle—the less dense material in the rising plume produces a broad negative anomaly; but the satellite passes closer to the excess mass in the elevated surface pushed up by the current, and the net gravity anomaly in the area over the rising current is positive.' However, the virtual indifference of anomalies in geoid shape to continental masses illustrates that there is little correlation with surface elevation [*Stacey*, 1969; *Kaula*, 1972]. It is also noted that the geoidal anomalies are generally positive over both spreading ridges and trenches [*Kaula*, 1972].

Kaula [1972, p. 393] mentioned five factors that can influence the existence of a mass excess in a steady-state flow system: (1) the piling up of material at the surface, (2) the replacement of less dense by more dense material at an interior interface, (3) thermal contraction, (4) transition to a denser phase, and (5) petrological fractionation in which a less dense component is separated from the material before it enters the region. These points are an almost literal description of the processes implied by our model of gravitational anchors. The total mass builds up because the tholeiitic fractions are carried away from the center of downwelling by plate motion.

Another point made by Kaula seems particularly apt in view of our description of the melting anomaly as a throttling point adjacent to a region of downwelling (stagnation of horizontal flow). He stated [*Kaula*, 1972, p. 393], 'The greater effectiveness of lateral transfer also suggests that stagnation points (regions where the flow changes direction, such as ocean rises or trench and island arcs) will tend to be regions of gravity excess, while regions dominated by horizontal flow will tend to be regions of gravity deficiency.'

All the above comments obviously show that qualitative dynamic interpretations of gravity data are ambiguous. Our main point, however, is that the data are at least as consistent with a downwelling model as an upwelling model, and in our opinion the geoidal anomaly is explained more reasonably by the effects of accumulation of dense mantle residua.

Density models of the oceanic mantle. *Ringwood* [1972] recently summarized experimental evidence on the chemistry and mineralogical phase changes in the mantle. Ringwood believes the major part of the mantle to be pyrolite, a material with a 100 Mg/Mg + Fe ratio of 89 and a zero-pressure density (ρ_0) of 3.38 g cm^{-3}. We have previously discussed our ideas of fractionation in the asthenosphere source region, which, in our opinion, has much lower 100 Mg/Mg + Fe ratios. The melting process in the mantle beneath Hawaii tends to transfer low melting components laterally upward from its deeper zones into the melting region (that is, into the zone of maximum shearing gradients of Figure 2). Thus the migration of lowest melting factions essentially amounts to a diffusive enrichment of the upper part of the asthenosphere in iron, potassium, water, phosphorus, and other large minor elements, whether or not the entire asthenosphere is enriched in these materials. As we argued earlier, the refractory residua (or early crystalline products) associated with tholeiite melting have a higher range of 100 Mg/Mg + Fe ratios than the parental material but are denser than either their parental material or the underlying assemblage in the deeper mantle. Residual dunite has an average 100 Mg/Mg + Fe ratio of 84.6 and a ρ_0 of at least 3.40 g cm^{-3}. The density of this material is therefore at least 0.02 g cm^{-3} greater than that of pyrolite.

Wang [1970] showed that an internally consistent model for bulk sound velocity versus density in the mantle fits experimental velocity data for Twin Sisters dunite (100 Mg/Mg + Fe = 93; mean atomic weight $m = 21.0$) in the upper mantle but deviates in the lower mantle toward assemblages with mean atomic weights in the range 21.3–21.5. Wang suggested, therefore, that the entire mantle may not have a very wide range of iron contents (for 100 Mg/Mg + Fe = 0, $m = 29.1$). The family of models derived by *Press* [1972, Figure 24], using Monte Carlo methods, substantiate Wang's general conclusions.

Clearly there is as yet no complete agreement on variations in iron content with depth in the mantle [*Wang*, 1970; *Anderson et al.*, 1972; *Ringwood*, 1972], but there seems to be growing evidence that something like Wang's model describes the general trend of relationships between bulk sound velocity, density, and mean atomic weight [*Wang*, 1972, Figure 10]. The mean atomic weight for 100 Mg/Mg + Fe = 84.6 olivine is 21.5, which is at the upper limit of the range of Wang's results for the lower mantle.

The model of descending density currents of residual phases enriched in iron suggests that there are probably lateral heterogeneities in the composition of the lower mantle. The family of successful solutions by *Press* [1972, Figure 24] suggest that densities could vary as much as ± 0.1 or 0.2 g cm^{-3}. This is also approximately the range of deviations to be expected for variations in mean atomic weight corresponding to olivine compositions between 100 Mg/Mg + Fe = 93 (Twin Sisters dunite) and

100 Mg/Mg + Fe = 84.6 (residuum from Hawaiian tholeiite melting).

Iron enrichment of the sinking residua below melting anomalies of Hawaiian type also has important implications concerning maintenance of the proposed density currents across depths of high-pressure phase transformations. The important experimental work of Ringwood on high-pressure phase transitions (see summary in *Ringwood* [1972, Figure 6]) has convincingly demonstrated that pyroxene and olivine begin to progressively transform to garnet and spinel-type phases, respectively, at depths between 300 and 400 km. The phase diagram for the system Fe_2SiO_4-Mg_2SiO_4 [*Ringwood*, 1972, Figure 4] shows that the spinel transitions begin at lower pressures in more iron-rich olivines.

The pressure difference of the transition for a change from a 100 Mg/Mg + Fe ratio of 93–84.6 is more than 10 kb, implying that transitions within the sinking residua of tholeiite melting would begin some 30 km or more above the transition depth for the more magnesian mantle compositions. Thus we would expect a cascading density effect within the stream tube that tends to offset the effect of increasing viscosity with depth on the velocities of descent.

Seismic wave paths in the deep mantle. Kanasewich et al. [1973] and *Julian and Sengupta* [1973] have independently reported evidence of anomalous phase velocities for seismic wave paths that traverse the deepest few hundred kilometers of the mantle. Such wave paths that travel beneath the position of Hawaii were found in the study by *Kanasewich et al.* [1973, Figure 4] to show anomalously high phase velocities; this study reported wave velocities about 0.3 km sec^{-1} higher than velocities for P waves in model 2 of *Birch* [1964], the deviation beginning at a depth of about 2,600 km (the core-mantle boundary is at about 2,900 km). On the other hand, *Julian and Sengupta* [1973] indicated a region of low phase velocities near Hawaii and anomalously high velocities to the northwest.

Both of the above studies emphasized the correlation between anomalous wave paths and the location of Hawaii and suggested the possibility that the seismic data have sampled properties in the mantle that are in some way related to Morgan's hypothesis of thermal plumes. We suggest, on the contrary, that these anomalies may be more consistent with the existence, position, and dimensions of the foot of a gravitational anchor beneath Hawaii. Although the relation may be accidental, it is noted that the velocity deviations shown by *Kanasewich et al.* [1973] are of approximately the same magnitude as those caused by the range of composition variations discussed in the preceding section. It is recognized that, on the existing evidence, interpretation of such velocity anomalies may be ambiguous and controversial, but, as was the case with the gravity data, the present model is no less consistent with available data than the plume model.

Bathymetry and heat-flow data. The bathymetric profile shown in Figure 3 [*Uspensky*, 1972] shows that the ocean floor east of Hawaii is systematically deeper than the floor west of Hawaii. The average difference is somewhat less than a kilometer. However, note that the maximum depths occur a few hundred kilometers east of the Hawaiian Deep. Although there are other possible explanations, the general bathymetric discontinuity is of roughly the correct magnitude for the pressure effects discussed in the appendix (section 2).

The above discontinuity in average depth is shown in the profile of apparent densities in the upper 50 km of the earth computed by *Uspensky* [1972, Figure 4]. In the same figure he also summarized heat flow data across the Pacific. There is clearly a systematic decrease in heat flow from the region of the East Pacific rise to roughly the position of Hawaii, west of which there is little change. It seems to us that this profile is consistent with the thermosiphon concept discussed in section 3 of the appendix and not with the idea that Hawaii represents a hot spot fed by thermal plumes. Certainly there is no anomaly of regional heat flow such as is seen in the vicinity of spreading ridges. If anything, the heat flow in the immediate vicinity of Hawaii is lower than that in adjacent regions. As we pointed out earlier, in agreement with conclusions of *Schubert and Turcotte* [1972], the contribution of viscous dissipation in asthenospheric flow to the surface flux is approximately constant. Volcanism in Hawaii actually represents a heat leak relative to the average flux, and consequently such an anomaly would be more of a cold spot than a hot spot of regional surface flux. However, the effect of thermal feedback is to accelerate flow in the upper part of the asthenosphere at the melting anomaly, thereby compensating the volcanic heat loss.

IMPLICATIONS OF GRAVITATIONAL ANCHORS

Kinematics of the Pacific mantle. Gravitational anchors satisfy all the available evidence suggesting that melting anomalies of the type that produce linear island chains have remained in roughly the same positions relative to the deep mantle over at least the latest 40 m.y. and probably the latest 100 m.y. In fact, we suggest that the 'anchor' concept provides a far more sensitive inertial guidance system for positioning of melting anomalies than does the concept of thermal plumes. This is because the anchor is localized at a level just below the site of melting, not 2,800 km deeper. Density currents, of either positive or negative sign, tend to be divergent at their leading ends. This effect has been postulated by *Morgan* [1972*a*, *b*] and others as providing a tractive force for plate motion. However, by the very nature of such divergence, the rising plume loses its coherence as a focusing mechanism. Typically, it would be expected that the head of the plume would break up into swirls and various forms of substructures as it impinges on the lithosphere in a situation such as that below Hawaii. Similar instabilities will affect downgoing density currents, but they do not influence the sharpness and linearity of related volcanism. They will, however, affect the size and position of the accumulating residuum at the level of stable stratification.

Although the anchoring effect of the density current tends to lock associated melting anomalies to the underlying mantle, some drift can probably occur as a consequence of accelerations of the melting wave in the asthenosphere by thermal feedback [*Shaw*, 1973]. However, the inertial effect of the anchor counteracts this tendency by reestablishing a more symmetrical flow field during intervals of low propagation rates. Such swings around the anchor could well account for the apparent slow movement of melting anomalies with time [*Molnar and Atwater*, 1973; *Clague and Jarrard*, 1973*a*].

The above considerations suggest the possibility that propagation directions of linear volcanic chains could well be reversed relative to the Hawaiian direction, depending on balances between velocities of asthenospheric transport and the sinking velocity of the anchor. This may indeed be the case in the Austral Islands, where ages appear to decrease in both directions from Rurutu toward both Jaluit Island and Macdonald seamount [*Krummenacher and Noetzlin*, 1966; *Clague and Jarrard*, 1973*b*]. Conceivably, an episode of very fast sinking could even break the continuity of a stream tube (analogous to drop formation by fluctuations of flow rates in a laminar jet). This effect would then produce an offset in the inertial position of the melting anomaly.

On present evidence we find no conflict between our model and descriptions of volcanic lineaments such as the Hawaiian ridge as 'aseismic ridges' [*Wilson*, 1963]. As was discussed by *Morgan* [1965], *Weertman* [1970], and many others, the flow law at stress levels implied by the size and density contrast between the downgoing residuum and surrounding mantle is controlled by diffusive processes. A smooth variation of creep rates is to be expected, particularly since this material has been stripped of its low-melting and volatile constituents. Other transitions, such as olivine → spinel, take place gradually over a range of pressures in multicomponent assemblages [*Ringwood*, 1972], so that sudden volume changes are not expected. However, we do not rule out the possibility that occasional seismic events could be associated with the proposed mechanism.

Plate motion in time. Because the gravitational anchor is decoupled from the lithosphere by the zone of asthenospheric melting, it has no substantial influence on plate motion (unless there were enough such melting anomalies to significantly influence the average rate of asthenospheric transport toward spreading ridges). The anchors essentially represent pinning points of the melting anomaly relative to the mantle below the asthenosphere. Times of change in spreading directions simply pivot about these markers unless the lull in melting rates is long enough to permit the density current to become totally detached from the zone of melting. However, as the rate of supply of residuum decreases, so does the diameter of the stream tube. Therefore there is a tendency for the sinking rate to slow at times of low rates of lithosphere-asthenosphere counterflow.

Birth of an anchor. As is the case with most forms of convectional instability, the point of origin of stream tubes depends on the existence of some disturbance of the previously existing flow field. As was pointed out by *Shaw* [1973], lateral chemical and temperature heterogeneities in the mantle will have a major influence on the location and nature of a melting anomaly. However, it is tempting to speculate that there is some systematic relationship among the locations, number, timing, and productivity of melting anomalies, particularly those associated with linear island chains in the Pacific.

The thermal structure of the asthenosphere implied by the thermosiphon concept (section 3 of the appendix) suggests that the most favorable regions for development of melting anomalies of Hawaiian type are near spreading ridges. Either of two simple reasons can explain why such anomalies are now seen in the central Pacific: either there is a major change in mantle composition between Hawaii and the East Pacific ridge or the melting anomaly originated at the ridge, and the center of spreading has moved east relative to the pinning point. The latter could be tested by comparisons of ages at the origin of a linear volcanic chain and the associated magnetic anomaly related to spreading rates. Unfortunately, the origin of the Hawaiian-Emperor system is lost in the complexity of the Aleutian trench system, and other linear volcanic chains are not known in similar detail. The Society Islands are interesting in this context, since they may well be a melting anomaly of the line island type that does not appear to extend back beyond a bend, nor are they presently near a spreading ridge.

If melting anomalies of the Hawaiian type indeed begin below central regions of the Pacific plate, there must be some heterogeneity of compositions, melting temperatures, or stresses of lithosphere-mantle coupling that initiate surface volcanism. It is pointed out by *Lachenbruch* [1973*b*] that stresses in the lithosphere and asthenosphere will be influenced significantly by asthenosphere melting. In our view, there are always significant and time-dependent variations of such coupling stresses from place to place over the Pacific, even though plate motion is on the whole fairly steady. The uncertainties of mechanical properties of solid state assemblages versus their melting temperatures make it difficult to say whether volcanism would begin at a position of anomalously high stress, or because the secular accumulation of a melt fraction would happen to satisfy the mechanical criteria of extensional failure. We note, as pointed out by *Secor* [1965], that the difference between the greatest and the least principal stresses must be fairly small, or failure would occur in a shear mode rather than by extensional injection of a fluid phase. Therefore, as was given in the introductory outline of events, we think that anomalous stress effects of the type proposed by *Lachenbruch* [1973*b*] are important steps in the feedback model but that perpetuation of volcanic fracture systems occurs because of accumulation of melt to some critical fraction. Admittedly this is something of a 'chicken-egg' distinction when it is viewed within the context of a dynamic feedback system.

In our judgment, there is nothing inconsistent between the idea of ridge spreading by broad upwelling of partially molten material [*Lachenbruch*, 1973*a*] and anchoring of Hawaiian type anomalies by downwelling of iron-rich residua. The downwelling model is more localized and proceeds in general at higher local flow velocities. Therefore there is no reason why the downwelling cannot also penetrate a region of slower upwelling of less dense materials. In our view, the main difference between the Hawaiian melting anomaly and the Iceland melting anomaly could relate to the symmetry of flow about the point of downwelling and the global balances of plate motion and ridge spreading that govern the kinematic motion of spreading centers relative to the gravitational anchors. If so, Iceland is simply a symmetrical form (that is, nonpropagating) of our general dynamic model and contains a gravitational anchor beneath the melting anomaly there. If the existence of the V-shaped lineaments described by *Vogt* [1971] south of Iceland are proved by dating of dredge samples to confirm the proposed propagation direction, it seems possible that this effect could simply relate to the expanding region of influence of counterflow and melting below Iceland.

It is noted that the depth to the core-mantle boundary is about 2900 km. The length of the Hawaiian ridge is about 3600 km, and the Emperor chain is roughly 3000 km. Therefore, if the density current has been operating since the origin of the Hawaiian-Emperor system, it would appear that an amount of residuum has accumulated at the core-mantle boundary about equal to the present volume of the gravitational anchor below Hawaii. This volume could be estimated from the volcanic volumes given by *Shaw* [1973] if the average ratio of melt to residual fractions were known. Assuming that the fraction of melt removed is roughly 10%, the volume of residuum is about an order of magnitude larger than the lava volume. This gives about 10^7 km^3 of residual material since the time of the Hawaiian-Emperor bend and suggests that the volume previously accumulated at the core-mantle boundary is of similar magnitude. Therefore the dimensions of the 'foot' of the density current in Figure 2 could be of the order 300 × 300 × 100 km, although its geometric form is entirely conjectural.

Angular velocity of rotation with depth in the earth. The thermal plume model of *Morgan* [1971, 1972*a*, *b*] assumes that the earth's mantle is in a state of rigid body rotation. An extensive global system of plumes rising at the velocities envisaged by *Morgan* [1972*a*, *b*] would eventually produce a major imbalance in distributions of angular momentum. This is because parcels of fluid moving up are subjected to a relative westward acceleration (that is, they are slowed relative to the mean rotation rate at the surface [*Shaw et al.*, 1971, p. 882] and vice versa for materials moving down). If the lower mantle were sufficiently fluid to sustain large regions of partial melting, it would seem likely that there would be a secular drift of the source regions to the east relative to the positions of related melting anomalies at the earth's surface. The same effect applies to our model, but in general the model implies a colder, less fluid mantle and involves much smaller total rates of vertical mass transfer. Furthermore, not all gravitational anchors are fed at such high rates as below Hawaii or Iceland. If the density-current model can be tied directly to seismic models of mantle structure, the relation may provide evidence on distributions of angular velocity in the mantle and rates of mantle-wide convection.

CONCLUSIONS

Given that melting processes beneath linear chains of shield volcanoes yield mantle residua that are more dense than their parental materials, and given the continuous shear interface between a rigid Pacific plate and a rheid asthenosphere, a self-perpetuating cycle of surface volcanism and downwelling residua appears dynamically inevitable. This model is consistent with currently available gravitational, bathymetric, and heat flow data and explains anomalously high *P* wave velocities in the deep mantle beneath Hawaii inferred by *Kanasewich et al.* [1973]. The plume hypothesis fails to explain the episodic nature of volcanism along the chains, the high *P* wave velocities, or the remarkably low heat flow gradients outside the very immediate vicinity of the volcanic edifice at the ends of the linear chains.

One of the main appeals of the plume hypothesis has been that, by definition, plume sites were fixed with respect to the lower mantle and thus could furnish a fixed reference system of plate motions. However, considerable evidence for the gradual drift of melting anomalies has recently been generated. The gravitational anchor, although relatively fixed by inertial forces, is controlled by an episodic process and may be expected to drift somewhat with time.

We wish to emphasize that we consider downwelling to be applicable to the origin of linear volcanic island chains and do not consider it to be a universal explanation for all terrestrial melting anomalies. It does not appear, for example, to be a promising mechanism for volcanism at mid-oceanic ridges, except in the case of anomalous areas like Iceland. It may, however, find application in the explanation of linear continental volcanic belts, such as those extending from the Columbia plateau to Yellowstone Park, and, within the framework of what is known of the geology of Mars, we consider that the downwelling hypothesis is as worthy of consideration as the plume hypothesis in speculations about the origin of the linear volcanic vents of Tharsis and Elysium [*Carr*, 1973].

APPENDIX: SOME FACTORS THAT INFLUENCE PRESSURE DISTRIBUTIONS AND TOPOGRAPHIC EXPRESSION OF MELTING ANOMALIES

1. *Adiabatic decompression.* If the melting instability is viewed in terms of changes of state across a throttling point, it can be alternatively expressed in terms of the Joule-Kelvin effect. *Waldbaum* [1971] has predicted very large increases of temperature in the mantle due to this effect, but it appears that he overestimated

the heating, because in his equation he used changes of total pressure rather than changes of fluid potential to compute temperatures. However, the results apply as stated for flow across a throttling point at a fixed level in the gravitational field. The magnitude of Joule-Kelvin coefficients for mantle materials is about 20°C/kb [*Waldbaum*, 1971, Table 1]. In the steady state this temperature and pressure change across a fixed position would correspond to a topographic depression of about 3 km ahead of the throttling point. This number remains uncertain, however, because the instability does not strictly resemble a simple throttle, and there are other effects of heat storage to take into account.

2. *Topographic effect of a sinking mass.* A pressure gradient as discussed above is also implied by the effect of a sinking mass. *Morgan* [1965] showed that the depression of the surface above a sinking sphere can be expressed as a combination of terms involving the pressure and velocity. From the point of view of gravity measurements, the 'pressure surface mass deficiency' and the mass excess of the sinker tend to cancel, so that the free air anomaly is mainly influenced by the velocity effect. This apparently predicts a negative free air anomaly in regions of horizontal convergence (such as at trenches and above the region of Figure 3 of this paper) and positive anomalies in regions of horizontal divergence (such as spreading ridges). However, Morgan pointed out that little reliance can be placed on numerical estimates, because of other factors.

Morgan [1965, p. 6180] gave the total depression above a sinking sphere in the form

$$h_{\text{tot}}(r) = HD^5/(D^2 + r^2)^{5/2}$$

where D is the depth to the center of the sphere, r is the horizontal distance from the vertical line through the sphere, and H is the maximum surface depression given by

$$H = 2\Delta\rho a^3/\rho D^2$$

For a density contrast $\Delta\rho \simeq 0.05$, the maximum depression would be about 1 km.

3. *Pressures implied by lithosphere-asthenosphere counterflow. Schubert and Turcotte* [1972] gave a one-dimensional analysis of symmetrical counterflow, incorporating temperature-dependent viscosities and effects of viscous dissipation on surface heat flux. Although we concur with their general approach, we think that the discussion of pressure gradients and topography is misleading. Figure 4 shows the model tested. Schubert and Turcotte assume that the velocity vector is horizontal and that therefore the pressure as a function of depth is hydrostatic, so that the surface elevation necessarily corresponds to the pressure gradient driving the flow. In a more complete model this might be true—for example, if the flow were driven by buoyancy forces generated in the asthenosphere below the descending slab. In this case, flow is driven by the total change in hydraulic head from the deep source to the center of spreading (the point of discharge), and the reversed topographic gradient between the ridge and trench has no effect on the flow of lithosphere (as with a siphon).

The one-dimensional model views the asthenosphere in a manner similar to that of a deformable pipe on a horizontal surface, where one end is at a faucet and the other is open. With the faucet on, the pressure gradient is a linear function of distance from the faucet, and the 'topography' of the upper surface of the pipe slopes down toward the point of discharge.

Although the model seems to be formally correct and internally consistent, it ignores other effects that control the general distribution of buoyancy forces in the mantle (it might be noted in Figure 4 that, if the lithosphere were treated as a fluid, albeit a much more

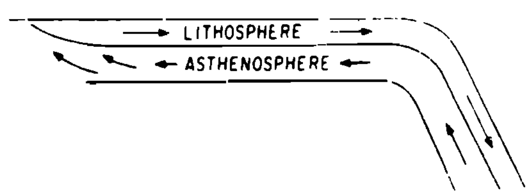

Fig. 4. One-dimensional model of lithosphere-asthenosphere counterflow [*Schubert and Turcotte*, 1972, Figure 1]. 'Model of shallow-mantle convection. Conservation of mass is satisfied by a counterflow in the asthenosphere at depths between 100 and 300 km. The return flow is driven by a hydrostatic pressure that increases with distance from the ridge. This pressure gradient is reflected as an increase in ocean-floor elevation away from the ridge' [*Schubert and Turcotte*, 1972, p. 946].

viscous fluid than the asthenosphere, the pressure gradient is reversed).

The model that appeals more to us is suggested by the idea of a thermosiphon. The concept is shown schematically in Figure 5.

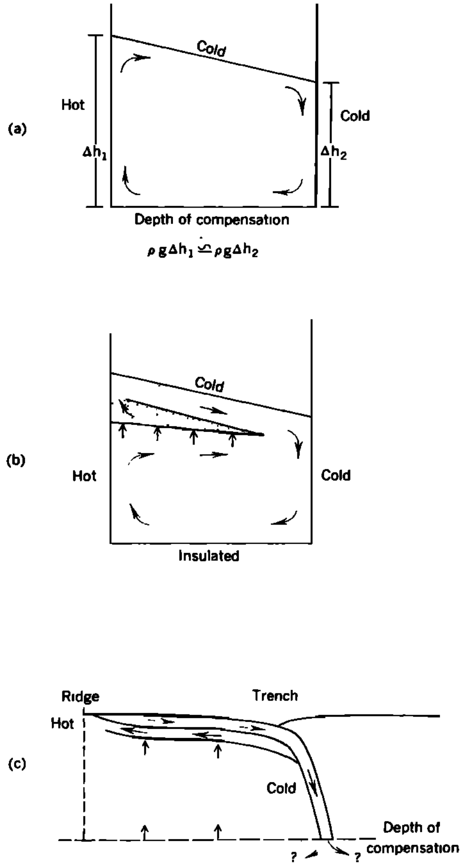

Fig. 5. Schematic model of asthenosphere based on convection driven by horizontal temperature gradients [*Allan et al.*, 1967; *McKenzie*, 1969] modified according to the thermosiphon concept proposed by *Shaw et al.* [1971, p. 882] (details of asthenosphere counterflow were not considered in this work of Shaw et al.). (*a*) Boundary layer flow of a viscous liquid in a container with one wall heated and another cooled; the surface is also cooled and the bottom is insulated. (*b*) Model as in (*a*) but of more highly viscous material with a low viscosity region generated by a heat source located somewhat below the surface. (*c*) Hypothetical thermosiphon model of lithosphere-asthenosphere counterflow. Material below the asthenosphere is continually displaced upward and heated by viscous dissipation. This material is also subject to sluggish clockwise overturn, as in (*b*).

Here, one vertical wall of a container partly filled with a viscous fluid is heated, the upper surface and opposite wall are cooled, and the bottom is insulated. If the viscosity is low enough, the convection is in the form of sharply defined boundary layers, but as viscosity increases the flow 'fills' the entire container so that the flow lines resemble those in the usual diagram of Benard convection, or as shown by *Schubert and Turcotte* [1972, Figure 3]. The model is similar to that for convection driven by a horizontal temperature gradient proposed by *Allan et al.* [1967] and applied by *McKenzie* [1969] to mantle convection.

The source of the 'hot wall' is not considered here; the horizontal temperature gradient is simply a fact based on profiles of heat flow across spreading ridges [*Sleep*, 1969; *McKenzie*, 1969; *Uspensky*, 1972]. If we now introduce concepts of viscous heating and strong gradients of viscosity in Figure 5*a*, the flow pattern can be drastically modified on the local scale while the same sense of general circulation is maintained. For example, if the fluid is in general highly viscous and a heater is introduced in the stippled region of Figure 5*b*, a relatively fluid lens is generated between the cold surface layer and the deep circulation. The combination of additional buoyancy forces and traction of the underlying circulation would quickly squeeze this fluid out at the apex of the fluid surface if it were not continuously regenerated by heating new increments of the underlying fluid.

In most of the present models of asthenospheric transport, whether that of *Schubert and Turcotte* [1972], *Shaw* [1973], or others, the asthenosphere is recognized as a region in which there are sharp maximums of viscous dissipation (compare *Schubert and Turcotte* [1972, Figure 2] and *Shaw* [1973, Figure 8]); this would also be true if the lithosphere were 'dragged along' by traction from an underlying convection cell. Therefore a situation analogous to Figure 5*b* may be the most appropriate one. If so, general counterflow of the asthenosphere is simply a displacement of the more sluggish circulation in the deeper mantle. This model is shown in Figure 5*c*. Here there will also be a lateral temperature gradient in the asthenosphere and a gradual incorporation of underlying mantle into the region of asthenosphere transport and melting. The 'gravitational anchors' below melting anomalies such as Hawaii are viewed as a local penetration or disturbance of the general circulation.

Although the thermosiphon model is difficult to model in numerical detail, it appears to be conceptually the most consistent with profiles of heat flow, topography, and density across the Pacific summarized recently by *Uspensky* [1972, Figures 3, 4].

Acknowledgments. We thank our colleagues A. H. Lachenbruch and D. P. Hill for critically reviewing the manuscript.

Publication authorized by the Director, U.S. Geological Survey.

REFERENCES

Allan, D. W., W. B. Thompson, and N. O. Weiss, Convection in the earth's mantle, in *Mantles of the Earth and Terrestrial Planets,* edited by S. K. Runcorn, pp. 507-512, Interscience, New York, 1967.

Anderson, D. L., C. Sammis, and T. Jordan, Composition of the mantle and core, in *The Nature of the Solid Earth,* edited by E. C. Robertson and others, pp. 41-66, McGraw-Hill, New York, 1972.

Betz, F., Jr., and H. H. Hess, The floor of the North Pacific Ocean, *Geogr. Rev., 32,* 99-116, 1942.

Birch, F., Density and composition of the mantle and core, *J. Geophys. Res., 69,* 4377-4388, 1964.

Bradley, W. H., Vertical density currents, *Science, 150,* 1423-1428, 1965.

Bradley, W. H., Vertical density currents, *Limnol. Oceanogr., 14,* 1-3, 1969.

Carr, M. H., Volcanism on Mars, *J. Geophys. Res., 78,* 4049-4062, 1973.

Clague, D. A., and R. D. Jarrard, Hot spots and Pacific plate motion (abstract), *Eos Trans. AGU, 54,* 238, 1973*a*.

Clague, D. A., and R. D. Jarrard, Tertiary Pacific plate motion deduced from the Hawaiian-Emperor chain, *Geol. Soc. Amer. Bull., 84,* 1135-1154, 1973*b*.

Deer, W. A., R. A. Howie, and J. Zussman, *Rock Forming Minerals,* vol. 1, p. 22, John Wiley, New York, 1962.

Dicke, R. H., Average acceleration of the earth's rotation and the viscosity of the deep mantle, *J. Geophys. Res., 74,* 5895-5902, 1969.

Eaton, J. P., Crustal structure and volcanism in Hawaii, in *The Crust of the Pacific Basin, Geophys. Monogr. Ser.,* vol. 6, edited by G. A. Macdonald and Hisashi Kuno, pp. 13-29, 1962.

Eaton, J. P., Evidence on the source of magma in Hawaii from earthquakes, volcanic tremor, and ground deformation (abstract), *Eos Trans. AGU, 48,* 254, 1967.

Forrester, J. W., *Principles of Systems,* pp. 5-7, Wright-Allen, Cambridge, Mass., 1968.

Goldreich, P., and A. Toomre, Some remarks on polar wandering, *J. Geophys. Res., 74,* 2555-2567, 1969.

Green, D. H., Composition of basaltic magmas as indicators of conditions of origin: Application to oceanic volcanism, *Phil. Trans. Roy. Soc. London, Ser. A, 268,* 707-725, 1971.

Green, D. H., and A. E. Ringwood, The stability fields of aluminous pyroxene peridotite and garnet peridotite and their relevance in the upper mantle structure, *Earth Planet. Sci. Lett., 3,* 151-160, 1967.

Gruntfest, I. J., Thermal feedback in liquid flow: Plane shear at constant stress, *Trans. Soc. Rheol., 7,* 195-207, 1963.

Happel, J., and H. Brenner, *Low Reynolds Number Hydrodynamics,* Prentice-Hall, Englewood Cliffs, N.J., 1965.

Hotz, P. E., and E. D. Jackson, X-ray determinative curve for olivines of composition Fo_{80-95} from stratiform and alpine-type peridotites, *U.S. Geol. Surv. Prof. Pap. 450-E,* E101-E102, 1963.

Jackson, E. D., and T. L. Wright, Xenoliths in the Honolulu volcanic series, Hawaii, *J. Petrol., 11,* 405-430, 1970.

Jackson, E. D., E. A. Silver, and G. B. Dalrymple, Hawaiian-Emperor chain and its relation to Cenozoic circumpacific tectonics, *Geol. Soc. Amer. Bull., 83,* 601-617, 1972.

Julian, B. R., and M. K. Sengupta, Seismic travel time evidence for lateral inhomogeneity in the deep mantle, *Nature, 242,* 443-447, 1973.

Kanasewich, E. R., R. M. Ellis, C. H. Chapman, and P. R. Gutowski, Seismic array evidence of a core boundary source for the Hawaiian linear volcanic chain, *J. Geophys. Res., 78,* 1361-1371, 1973.

Kaula, W. M., Global gravity and tectonics, in *The Nature of the Solid Earth,* edited by E. C. Robertson and others, pp. 386-405, McGraw-Hill, New York, 1972.

Kidd, W. S. F., K. Burke, and J. T. Wilson, The present plume population (abstract), *Eos Trans. AGU, 54,* 238, 1973.

Koyanagi, R. Y., and E. T. Endo, Hawaiian seismic events during 1969, *U.S. Geol. Surv. Prof. Pap. 750-C,* C158-C164, 1971.

Krummenacher, D., and J. Noetzlin, Ages isotopiques K/A de roches prélevees dans les possessions francaises de Pacifique, *Geol. Soc. France Bull., 8,* 173-175, 1966.

Lachenbruch, A. H., Differentiation and the gravitational driving force for material rising at an oceanic ridge, *J. Geophys. Res., 78,* 825-831, 1973*a*.

Lachenbruch, A. H., A simple mechanical model for oceanic spreading centers, *J. Geophys. Res., 78,* 3395-3417, 1973*b*.

McDougall, I., Volcanic island chains and sea floor spreading, *Nature, 231,* 141-144, 1971.

McKenzie, D. P., Speculations on the consequences and causes of plate motions, *Geophys. J. Roy. Astron. Soc., 18,* 1–32, 1969.

Menard, H. W., Gravity anomalies and vertical tectonics as indicators of plate motions (abstract), *Eos Trans. AGU, 54,* 239, 1973.

Molnar, P., and T. Atwater, Magnetic anomalies and evolution of the South Pacific: Implications for fixed hot spots (abstract), *Eos Trans. AGU, 54,* 240, 1973.

Morgan, W. J., Gravity anomalies and convection currents, *J. Geophys. Res., 70,* 6175–6204, 1965.

Morgan, W. J., Convection plumes in the lower mantle, *Nature, 230,* 42–43, 1971.

Morgan, W. J., Deep mantle convection plumes and plate motions, *Amer. Ass. Petrol. Geol. Bull., 56,* 203–213, 1972*a*.

Morgan, W. J., Plate motions and deep mantle convection, *Geol. Soc. Amer. Mem., 132,* 7–22, 1972*b*.

O'Hara, M. J., The bearing of phase equilibria studies in synthetic and natural systems on the origin and evolution of basic and ultrabasic rocks, *Earth Sci. Rev., 4,* 69–133, 1968*a*.

O'Hara, M. J., Are ocean floor basalts primary magma?, *Nature, 220,* 683–686, 1968*b*.

Press, F., The earth's interior as inferred from a family of models, in *The Nature of the Solid Earth,* edited by E. C. Robertson and others, pp. 147–171, McGraw-Hill, New York, 1972.

Ringwood, A. E., The chemical composition and origin of the earth, in *Advances in Earth Science,* edited by P. M. Hurley, pp. 287–356, MIT Press, Cambridge, Mass., 1966.

Ringwood, A. E., Mineralogy of the deep mantle: Current status and future developments, in *The Nature of the Solid Earth,* edited by E. C. Robertson and others, pp. 67–92, McGraw-Hill, New York, 1972.

Robie, R. A., P. M. Bethke, and K. M. Beardsley, Selected X-ray crystallographic data, molar volumes, and densities of minerals and related substances, *U.S. Geol. Surv. Bull.,* no. 1248, 62–63, 1967.

Schubert, G., and D. L. Turcotte, One-dimensional model of shallow mantle convection, *J. Geophys. Res., 77,* 945–951, 1972.

Secor, D. T., Jr., Role of fluid pressure in jointing, *Amer. J. Sci., 263,* 633–646, 1965.

Shaw, H. R., Rheology of basalt in the melting range, *J. Petrol., 10,* 510–535, 1969.

Shaw, H. R., Mantle convection and volcanic periodicity in the Pacific: Evidence from Hawaii, *Geol. Soc. Amer. Bull., 84,* 1505–1526, 1973.

Shaw, H. R., T. L. Wright, D. L. Peck, and R. Okamura, The viscosity of basaltic magma: An analysis of field measurements in Makaopuhi lava lake, Hawaii, *Amer. J. Sci., 266,* 225–264, 1968.

Shaw, H. R., R. W. Kistler, and J. F. Evernden, Sierra Nevada plutonic cycle, 2, Tidal energy and a hypothesis for orogenic-epeirogenic periodicities, *Geol. Soc. Amer. Bull., 82,* 869–896, 1971.

Sleep, N. H., Sensitivity of heat flow and gravity to the mechanism of sea floor spreading, *J. Geophys. Res., 74,* 542–549, 1969.

Spetzler, H., and D. L. Anderson, The effect of temperature and partial melting on velocity and attenuation in a simple binary system, *J. Geophys. Res., 73,* 6051–6060, 1968.

Stacey, F. D., *Physics of the Earth,* p. 51, John Wiley, New York, 1969.

Uspensky, D. G., Geological interpretation of gravity data for a profile across the Pacific Ocean, *J. Geophys. Res., 77,* 6316–6326, 1972.

Vogt, P. R., Asthenosphere motion recorded by the ocean floor south of Iceland, *Earth Planet. Sci. Lett., 13,* 153–160, 1971.

Waldbaum, D. R., Temperature changes associated with adiabatic decompression in geological processes, *Nature, 232,* 545–547, 1971.

Wang, Chi-yuen, Density and constitution of the mantle, *J. Geophys. Res., 75,* 3264–3284, 1970.

Weertman, J., The creep strength of the earth's mantle, *Rev. Geophys. Space Phys., 8,* 145–168, 1970.

Wilson, J. T., A possible origin of the Hawaiian Islands, *Can. J. Phys., 41,* 863–870, 1963.

Wilson, J. T., and K. Burke, Plate tectonics and plume mechanics (abstract), *Eos Trans. AGU, 54,* 238, 1973.

Wright, T. L., Chemistry of Kilauea and Mauna Loa lava in space and time, *U.S. Geol. Surv. Prof. Pap. 735,* 40 pp., 1971.

(Received June 22, 1973;
revised August 15, 1973.)